Nucleation and Global Time Scales in Ecological Invasion under Preemptive Competition

L. O'Malley[a], A. Allstadt[b], G. Korniss[a], and T. Caraco[b],

[a]Department of Physics, Applied Physics, and Astronomy, Rensselaer Polytechnic Institute, 110 8^{th} Street, Troy, NY 12180–3590, USA;
[b]Department of Biological Sciences, University at Albany, Albany, NY 12222, USA

ABSTRACT

The breakdown of biogeographic barriers allows some invasive species to reshape ecological communities and threaten local biodiversity. Most introductions of exotic species fail to generate an invasion. However, once introduction succeeds, invader density increases rapidly. We apply nucleation theory to describe spatio-temporal patterns of the invasion process under preemptive competition. The predictions of the theory are confirmed by Monte Carlo simulations of the underlying discrete spatial stochastic dynamics. In particular, for large enough spatial regions, invasion occurs through the nucleation and subsequent growth of many clusters of the invasive species, and the global densities are well approximated by Avrami's law for homogeneous nucleation. For smaller systems or very small introduction rates, invasion typically occurs through a single cluster, whose appearance is inherently stochastic.

Keywords: spatial competition, ecological invasion, nucleation theory

1. INTRODUCTION

Human-caused environmental changes have eroded natural barriers to the long-distance dispersal of plants and animals.[1] Consequently, expanding geographic ranges of invasive species have begun to homogenize the biota of different regions.[2] Successful exotic invaders often replace native species, and produce additional economic, epidemiological or agricultural problems in their new environments.[3] Many exotics, including certain species purposefully introduced by humans,[4] combine a low probability of establishment at each introduction with rapid population growth once introduction succeeds. Modeling introduction as a rare stochastic process, the conditions for homogeneous mixing and the applicability of the corresponding mean-field equations immediately break down. In this case either continuum[5] or discrete[6] (individual-based) spatial models are needed to address the problem.

In this paper we investigate a discrete spatial model for ecological invasion. Initially the spatial region is fully dominated by the "resident" species. The "invader" species is introduced stochastically where resources are locally available. The invader has an individual-level advantage over the residents, but the low probability of introduction, combined with a discrete spatial dynamics, can prevent the spread of the invader for extended times. Here we consider a model where the residents and the competitively superior invaders compete for a common limiting resource preemptively.[7–10] We demonstrate that under these conditions, invasion is governed by nucleation and growth[11–14] of clusters of the invasive species. A relatively old empirical study[15] on primary ecological succession in sand-dune communities, where persistent vegetation (oak-pine forest) replaces colonizing grassland during succession, motivates our hypothesis that nucleation theory can explain important properties of biological invasion.

Further author information: Send correspondence to G.K., E-mail: korniss@rpi.edu

Fluctuations and Noise in Biological, Biophysical, and Biomedical Systems III, edited by Nigel G. Stocks, Derek Abbott, Robert P. Morse, Proc. of SPIE Vol. 5841 (SPIE, Bellingham, WA, 2005) · 0277-786X/05/$15 · doi: 10.1117/12.609267

2. THE MODEL

We consider an $L \times L$ lattice with periodic boundary conditions. Each site can be empty or occupied by a *single* individual (either a resident or an invader). A lattice site represents the minimal level of locally available resources required to sustain an individual organism, hence the "excluded volume" constraint. We introduce the local occupation numbers at site $\mathbf{x}$, $n_i(\mathbf{x}) = 0, 1$, $i = 1, 2$, representing the number of residents and invaders, respectively. By virtue of the excluded volume constraint, $n_1(\mathbf{x})n_2(\mathbf{x}) = 0$. New individuals can arise, where resources are available, by two distinct mechanisms. First, invaders are introduced randomly at empty sites. This spatially homogeneous stochastic process corresponds to a (typically weak) "background" capturing the effect of long-distance propagule dispersal. (In this paper we do not allow a similar process involving the resident species, but including immigration of resident individuals does not change the universal characteristics of the invasion dynamics since residents fully dominate the region initially.[16]) Second, new individuals of both species can be produced through *local* clonal propagation. That is, an individual occupying site $\mathbf{x}$ may reproduce if one or more neighboring sites are empty. (Most of the work presented here considers nearest-neighbor colonization only, but preliminary results with the inclusion of next-nearest neighbors are discussed in Sec. 5). Competition for resources, hence space, is preemptive; therefore, an occupied site cannot be colonized by either species until the current occupant's mortality leaves that site empty.

We performed dynamic Monte Carlo simulations to study the model. Our time unit is one Monte Carlo step per site (MCSS) during which L^2 sites are chosen randomly. If the site is empty, introduction or clonal propagation from the surrounding neighborhood can occur. The rate for introduction of an invader is β. The rate for colonization by species i occupying neighboring sites, is given by $\alpha_i \eta_i(\mathbf{x})$, where α_i is the individual-level colonization rate and $\eta_i(\mathbf{x}) = (1/\delta) \sum_{\mathbf{x}' \epsilon \mathrm{S}(\mathbf{x})} n_i(\mathbf{x}')$ is the density of species i around site $\mathbf{x}$. $\mathrm{S}(\mathbf{x})$ is the set of neighbors of site $\mathbf{x}$ and δ is the size of this neighborhood. (For nearest-neighbor colonization on a two-dimensional regular lattice, there are four such neighbors, δ=4.) If the site is occupied, the individual dies at rate μ (regardless of the species). We can summarize the local transition rules for an arbitrary site $\mathbf{x}$ as

$$0 \stackrel{\alpha_1 \eta_1(\mathbf{x})}{\longrightarrow} 1 \,, \quad 0 \stackrel{\beta + \alpha_2 \eta_2(\mathbf{x})}{\longrightarrow} 2 \,, \quad 1 \stackrel{\mu}{\longrightarrow} 0 \,, \quad 2 \stackrel{\mu}{\longrightarrow} 0 \,, \tag{1}$$

where $0, 1, 2$ indicates whether the site is empty, occupied by a resident, or an invader, respectively.

In the simulations, we initialized the system fully occupied by the resident species ($n_1(\mathbf{x})$=1 for all $\mathbf{x}$). We are interested in the parameter region where $\beta \ll \mu < \alpha_1 < \alpha_2$, so that introduction is a rare process, but the invaders have a reproductive-effort advantage. Then, due to mortality, the system quickly relaxes (much too fast for invader introduction to play a role) to the"quasi-equilibrium" state where the resident's population is balanced by its own clonal propagation and mortality rates (in the near absence of invaders). Throughout each simulation, we track the time-dependent global densities of the two species, $\rho_i(t) = (1/L^2) \sum_{\mathbf{x}} n_i(\mathbf{x}, t)$. We define the lifetime τ of the residents (also referred to as the invasion time) as the first passage time of the residents' global density to one-half of its quasi-equilibrium value ρ_1^*.

3. BASIC CHARACTERIZATION: SINGLE-CLUSTER AND MULTI-CLUSTER INVASION

As a result of rare introductions, individuals of the invasive species occasionally appear in the community. An invader lacking access to nearby resources may die without propagating. If a site opens in the local neighborhood (resource becomes available), the invader may colonize it. However, the empty site is likely surrounded by more than one resident. The resident's greater local density can compensate for its lower individual-level colonization rate, so the resident has the better chance of colonizing an empty site. Consequently, one expects small clusters of invaders to shrink and disappear. Residents, although weaker competitors, can prevail for some time, since preemptive competition imposes a strong constraint on the growth of the invaders. Invaders can succeed only if they generate a cluster sufficiently large (with a radius greater than a critical radius R_c) that it statistically tends to grow at its periphery.

Snapshots of configurations confirm the existence of a critical cluster size, beyond which the spread of the invader becomes statistically favorable. Further, we performed a special set of simulations, with appropriately

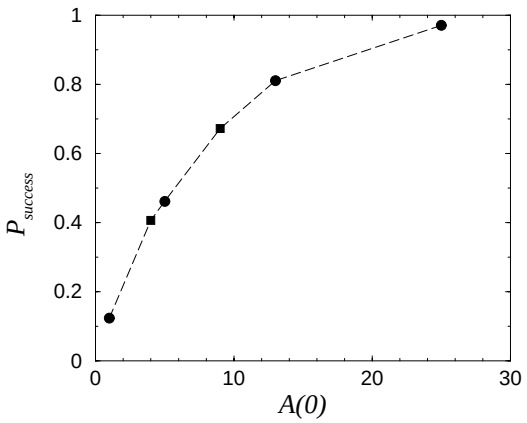

Figure 1. Success rate of an invasive compact cluster as a function of its initial cluster size $A(0)$ for L=128, α_1=0.70, α_2=0.80, and μ=0.10. Solid circles and squares represent the data for a "circular"-shaped and square-shaped initial invasive cluster on a lattice, respectively.

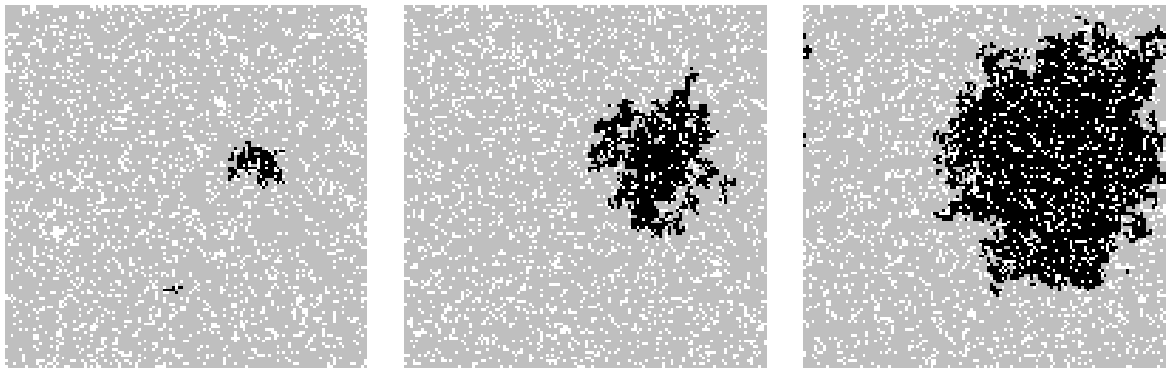

Figure 2. Configuration snapshots in the SC regime for β=10^{-6}, L=128, α_1=0.70, α_2=0.80, and μ=0.10. The three configuration snapshots, from left to right, correspond to time steps t = 1300 MCSS, t = 2000 MCSS, and t = 3000 MCSS. White represents empty sites, gray and black correspond to sites occupied by residents and invaders, respectively.

modified initial conditions and with further introduction suppressed (β=0), to obtain an estimate of the critical cluster size. We placed an initial single compact invader cluster of area $A(0)$ in the background of the equilibrium density of the residents, and measured the success rate $P_{success}$ for this cluster (out of 10,000 trials). For the parameter values used in this paper, we found that the success rate increases above 50% for an initial compact cluster of about nine sites, corresponding to R_c≈2 [Fig. 1]. Also, successful invasion becomes near certain for $A(0)$>25.

Snapshots also reveal strongly clustered growth of the invading species. For a given set of parameters, there exists a characteristic length scale R_o, the average spatial separation of invading clusters; for $L \ll R_o$ the invasion almost always occurs through the spread of a single invading cluster [single-cluster (SC) invasion], while for $L \gg R_o$ the invasion is the result of many invading clusters [multi-cluster (MC) invasion]. Conversely, fixing the linear system size L and other parameters (except the introduction rate), there is a characteristic value of β (now controlling R_o), such that for sufficiently low values of β, MC invasion crosses over to the SC pattern. These two different invasion modes, SC and MC, are illustrated by the snapshots in Fig. 2 and Fig. 3, respectively.

We also observe drastically different stochastic properties of the two invasion regimes, as can be seen from the time series of the global densities in Fig. 4. In the SC regime the appearance of the first (and almost always the only) successful invasive cluster is inherently stochastic [Fig. 4(a)]; the variance of the lifetime is comparable to its mean. In contrast, in the MC regime the global densities become self-averaging with a near-deterministic lifetime [Fig. 4(b)].

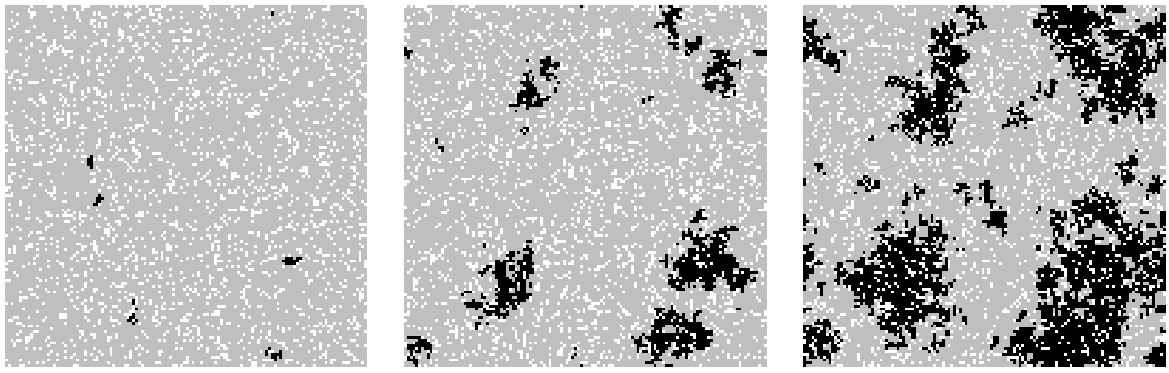

Figure 3. Configuration snapshots in the MC regime for β=10^{-4}, L=128, α_1=0.70, α_2=0.80, and μ=0.10. Note that all parameters are the same as in Fig. 2, except for β. The three panels, from left to right, correspond to time steps $t = 100$ MCSS, $t = 600$ MCSS, and $t = 1000$ MCSS. Sites are color coded as in Fig. 2.

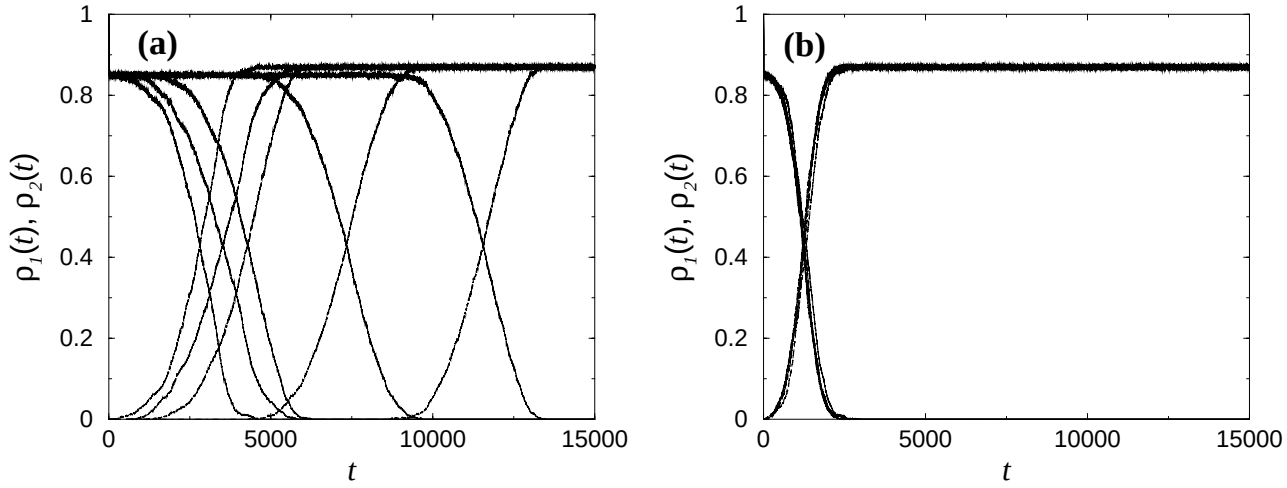

Figure 4. Five independent realizations of the time series of the two species' global densities during (**a**) SC invasion. Matching pairs of $\rho_1(t)$ and $\rho_2(t)$ intersect near a density of 0.425. (**b**) MC invasion. The parameters are the same as those in Fig. 2 and Fig. 3 for (**a**) and (**b**), respectively, i.e., L=128 for both, β=10^{-6} in (**a**) and β=10^{-4} in (**b**).

4. HOMOGENEOUS NUCLEATION AND GROWTH

The above picture suggests that one can apply the framework of homogeneous nucleation and growth[11–13] to describe the spatial and temporal characteristics of the spread of the invasive species. This framework, commonly referred to as KJMA[11–13] theory or Avrami's law, has successfully described analogous dynamic phenomena in ferromagnetic[17–20] and ferroelectric materials,[21,22] chemical reactions,[23] DNA replication,[24] and ecological systems.[16,25]

The simplest version of KJMA theory, in our ecological context, assumes that nucleation of an invading cluster is a Poisson process with nucleation rate per unit area I (constant in space and time). Further, it assumes that once a successful invading cluster has been nucleated, it grows deterministically with a constant radial velocity v. Since the derivation of KJMA theory is readily accessible in a number papers (see, e.g., Refs.[16,21]) including the original ones,[11–13] here we present only the results and a simple scaling argument[17,19] to obtain the governing time and length scales in the SC and MC regimes.

For small systems, $L \ll R_o$ (R_o to be determined later), invasion almost always occurs through the spread of a single invading cluster (the *first one* which nucleates and sweeps the system before another one appears)[16–18] (SC invasion). Since randomness appears only in the introduction (growth is assumed to be deterministic), the

statistics of the invasion times are related trivially to the underlying Poisson process. The cumulative probability of the invasion times $P_{\rm not}(t) = {\rm Prob}\{\tau > t\}$, i.e., the probability that the resident's global density has not decayed to $\rho_1^*/2$ by time t, has an exponential distribution

$$P_{\rm not}(t) = \begin{cases} 1 & \text{for } t \le t_g \\ \exp[-(t-t_g)/\langle t_n\rangle] & \text{for } t > t_g \end{cases} , \tag{2}$$

where $\langle t_n\rangle = [L^2 I]^{-1}$ is the average nucleation time and $t_g \sim L/v$ is the deterministic growth time until the invasive species dominates half of the system. For very small nucleation rates per unit area, the lifetime of the resident species is governed by the large average waiting time until the the first successful invader cluster nucleates, hence $\langle\tau\rangle = \langle t_n\rangle + t_g \approx \langle t_n\rangle$.

For large systems, $R_o \ll L$, many stochastically nucleated and growing invader clusters contribute to the extinction of the resident (MC invasion). In the limit of $L \to \infty$, the invasion process becomes self averaging: $P_{\rm not}(t)$ approaches a step function (centered at a system-size independent lifetime $\langle\tau\rangle$) and the global densities approach deterministic functions. In this limit, $R_c \ll R_o \ll L$, in two dimensions, the density of the resident species is given by KJMA theory[11–13] or Avrami's law

$$\rho_1(t) = \rho_1^*\, e^{-\ln(2)(t/\langle\tau\rangle)^3} . \tag{3}$$

The scaling behavior of the self-averaging, system-size independent lifetime $\tau{\equiv}\langle\tau\rangle$ in two dimensions can be argued as follows.[17,19] The average diameter of the invading clusters at time $t{=}\tau$ scales as $v\tau$, and can also be seen as the average spatial separation between such clusters, thus $R_o \sim v\tau$. Further, at the same instant, on average, one cluster has been nucleated in a corresponding area of diameter R_o, thus $IR_o^2\tau \sim 1$. Hence, one obtains

$$\tau \sim (Iv^2)^{-1/3} , \tag{4}$$

and

$$R_o \sim \left(\frac{v}{I}\right)^{1/3} \tag{5}$$

for the characteristic time and length scales of the system in the limit of $L \to \infty$. Also note that Eqs. (4) and (5) are also the only time and length scales that can be constructed by dimensional analysis in the MC regime. Further, as can be seen from Eq. (4), the microscopic parameters of a specific model (the local rates β, α_i, μ, and δ in our ecological model) govern the characteristic time scale (the lifetime τ) through their impact on both the nucleation rate per unit area I and the radial growth velocity v.

5. RESULTS AND DISCUSSION

While local introduction is a Poisson process, lacking a Hamiltonian or an effective free energy for the model, it is not known *a priori* whether the nucleation of a "supercritical" cluster will also be Poisson. To this end, in the SC regime, we constructed cumulative probability distributions for the lifetime of the resident species $P_{\rm not}(t)$, i.e., the probability that the global density of the resident has not crossed below $\rho_1^*/2$. We found that these distributions are indeed exponentials in accordance with Eq. (2) (indicating that the nucleation of a successful invading cluster is a Poisson process). We show results for a fixed (sufficiently small) system size for three introduction rates in Fig. 5(a). From the slopes of the exponentials we obtained the average nucleation times [Fig. 5(b)], hence the β-dependence of the nucleation rate per unit area $I(\beta)$. Since $\langle t_n\rangle = [L^2 I(\beta)]^{-1}$, we conclude that $I(\beta) \sim \langle t_n\rangle^{-1} \sim \beta$. In the SC regime, the invasive spread is inherently stochastic; it is initiated and completed by the first randomly nucleated successful cluster of the invasive species. For very low values of β, the lifetime is dominated by the very large average nucleation times, hence

$$\langle\tau\rangle = \langle t_n\rangle + t_g \approx \langle t_n\rangle \sim \beta^{-1} , \tag{6}$$

as can also be seen in Fig. 5(b).

In the MC regime we applied Avrami's law, Eq. (3), to approximate the functional form of the time-dependent global density of the resident species. Our results in Fig. 6(a) show that it is, indeed, a very good approximation

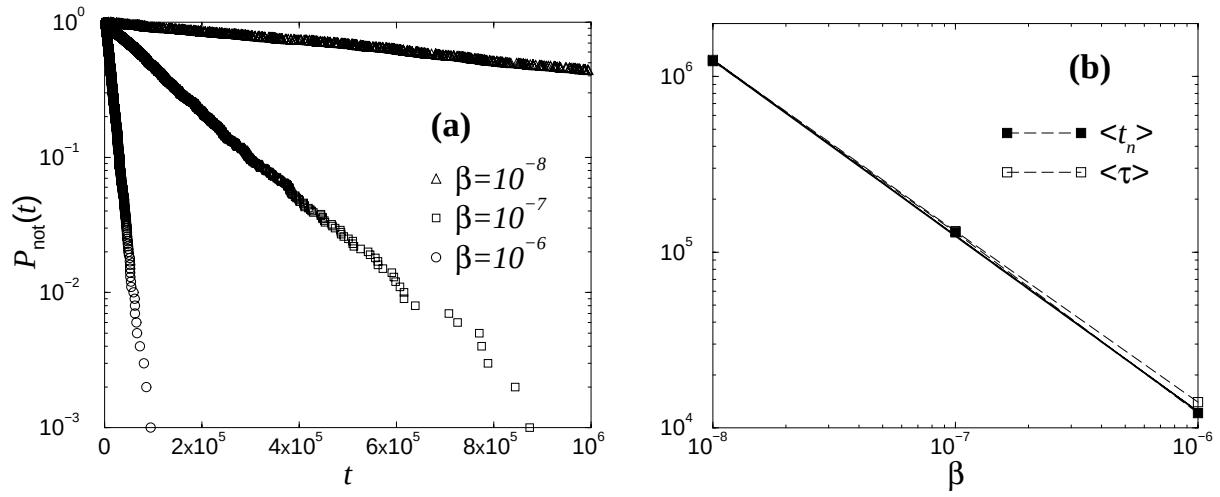

Figure 5. (**a**) Cumulative probability distributions $P_{\rm not}(t)$ on log-linear scales for L=64, α_1=0.70, α_2=0.80, and μ=0.10 for three different values of β (in increasing order from the top). (**b**) Average nucleation time and average lifetime (in units of MCSS) vs. the introduction rate on log-log scales for the same L, α_1, α_2, and μ as in **(a)**. The straight solid line corresponds to a slope -1, indicating $\langle t_n\rangle \sim \beta^{-1}$ in the SC regime.

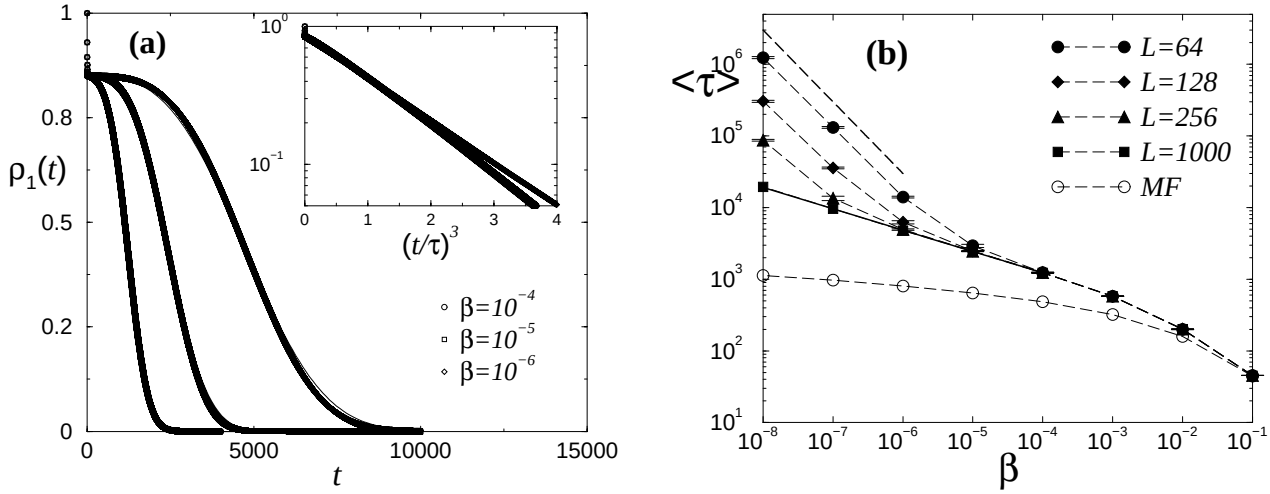

Figure 6. (**a**) Time-dependent global density of the resident species $\rho_1(t)$ in the MC regime for L=1,000, α_1=0.70, α_2=0.80, and μ=0.10, for three different values of the introduction rate β (in increasing order from the top). The solid curves represent Avrami's law, Eq. (3), using the measured lifetime $\langle\tau\rangle$ as the only parameter. The inset shows $\rho_1(t)$ vs. $(t/\langle\tau\rangle)^3$ on log-linear scales. (**b**) Average lifetime (in units of MCSS) vs. the introduction rate rate on log-log scales for the same α_1, α_2, and μ as in **(a)**. The straight solid line (across the L=1000 system data points) is the best fit power-law indicating $\langle\tau\rangle \sim \beta^{-0.30}$ in the MC regime. The straight dashed line corresponds to a slope -1, indicating the β-dependence of the average lifetime in the SC regime, Eq. (6). For comparison, we show the lifetime of the mean-field (MF) model, obtained by numerically integrating the mean-field rate equations defined by the rates in Eq. (1).

for times $t \leq \langle\tau\rangle$. Assuming that the spreading velocity of the invading clusters is constant and using our results from the SC regime that $I(\beta) \sim \beta$, KJMA theory Eq. (4) predicts that

$$\langle\tau\rangle \sim [I(\beta)]^{-1/3} \sim \beta^{-1/3} \tag{7}$$

in the MC regime. The measured exponent, -0.30, is not too far off [Fig. 6(b)], but it indicates that the assumption of a constant spreading velocity (possibly as a result of the nontrivial surface properties of the

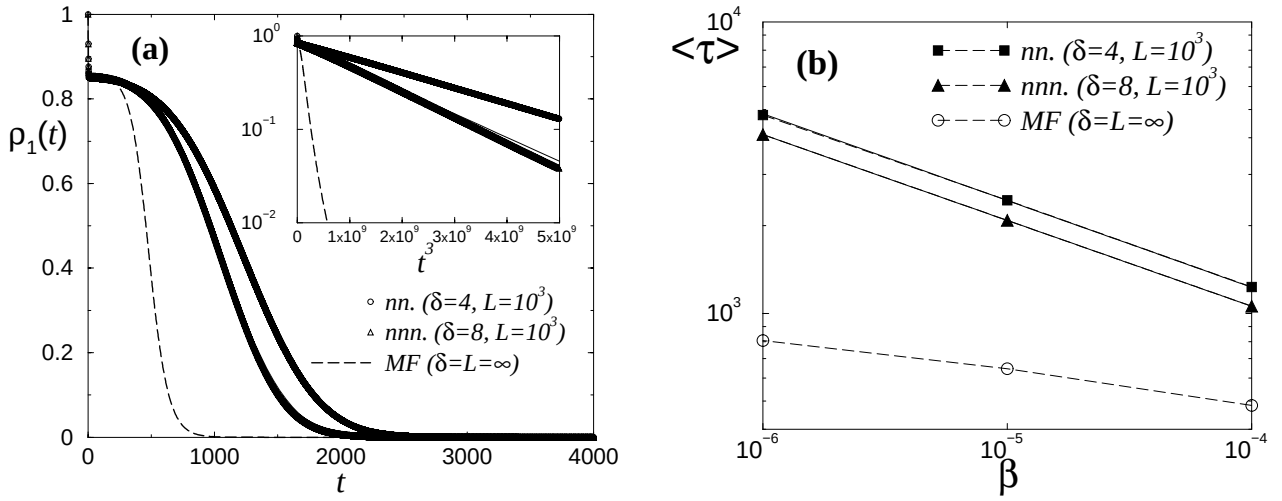

Figure 7. (**a**) Comparison of the global time-dependent density of the resident species $\rho_1(t)$ in the MC regime with nearest-neighbor ($\delta = 4$) and next-nearest-neighbor ($\delta = 8$) colonization. In both cases $\beta = 10^{-4}$, L=1,000, α_1=0.70, α_2=0.80, and μ=0.10. The solid curves represent Avrami's law, Eq. (3), using the measured lifetime $\langle\tau\rangle$ as the only parameter. For comparison, the mean-field (MF) time-dependent density for these rates is also shown. The inset shows $\rho_1(t)$ vs. t^3 on log-linear scales. (**b**) Average lifetime (in units of MCSS) vs. the introduction rate rate on log-log scales for nearest-neighbor and next-nearest-neighbor colonization in the MC regime for the same α_1, α_2, and μ as in **(a)**. The straight solid lines (across the L=1000 system data points) are the best fit power-laws, indicating $\langle\tau\rangle \sim \beta^{-0.30}$ for both cases.

clusters) may break down.

To study the robustness of the KJMA-type nucleation in our ecological model, we implemented additional simulations with next-nearest-neighbor colonization ($\delta = 8$). The corresponding global densities are qualitatively similar to the nearest-neighbor case ($\delta = 4$); the shape of the resident's decaying density is still well approximated by Eq. (3) up to the lifetime when effects of coalescing clusters become important [Fig. 7(a)]. Further, the lifetime $\langle\tau\rangle$ exhibits the same scaling with the introduction rate $\langle\tau\rangle \sim \beta^{-0.30}$ [Fig. 7(b)]. The neighborhood size seems to directly affect the radial growth velocity, and through it, the actual value of the lifetime.

6. SUMMARY AND OUTLOOK

We studied invasive spread in a two-species ecological model with preemptive competition, assuming that introduction of the favored species is a rare stochastic process. We found that nucleation theory, in particular Avrami's law, describes this phenomenon very well. Figure 6(b) essentially summarizes our findings. For infinitely large systems and sufficiently small β ($\beta < 10^{-3}$ for our choice of the other parameter values) the system exhibits MC invasion and is well approximated by Avrami's law. The lifetime is self-averaging and scales as $\langle\tau\rangle \sim \beta^{-0.30}$. For larger β, due to the almost immediate coalescing of the clusters, nucleation theory breaks down; in fact the mean-field approximation begins to work much better as a result of the almost immediate mixing of small clusters. For any finite system, however, there is a sufficiently small value of β such that $R_o > L$ and the invasion crosses over to SC mode. For example, for L=128 this crossover occurs at around $\beta = 10^{-6}$, while for L=256 at around $\beta = 10^{-7}$. For β less than these values, the invasion is inherently stochastic and the average lifetime scales as $\langle\tau\rangle \sim \beta^{-1}$, reflecting the underlying Poisson process for nucleating a successful invading cluster.

Further analyses of the spatially structured dynamics of ecological rarity should advance our understanding of exotic invasions, and also contribute to basic knowledge in evolutionary biology and epidemiology. Systematic studies of the critical cluster size and the cluster-size dependence of the spreading velocity are under way. The structure of the spreading clusters, in particular, the roughness of their surface, is expected to play an important role in the latter.

ACKNOWLEDGMENTS

Discussions with M.A. Novotny, P.A. Rikvold, and J.A. Yasi are greatfully acknowledged. We also thank Z. Toroczkai for helping us implement a numerical integrator routine for the mean-field approximations. This research is supported in part by NSF through Grant Nos. DMR-0113049, DMR-0426488, DEB-0342689 and by the Research Corporation through Grant No. RI0761.

REFERENCES

1. J.S. Dukes, H.A. Mooney, *Trends Ecol. Evol.* **14**, 135 (1999).
2. J.D. Olden, N.L. Poff, M.R. Douglas, M.E. Douglas, K.D. Fausch, *Trends Ecol. Evol.* **19**, 18 (2004).
3. D. Pimentel, L. Lach, R. Zuniga, D. Morrison, *BioScience* **50**, 53 (2000).
4. C.J. Veltman, S. Nee, M.J. Crawley, *Am. Nat.* **147**, 542 (1996).
5. J.D. Murray, *Mathematical Biology I and II, 3rd edition* (Springer-Verlag, New York, 2002, 2003).
6. R. Durrett and S.A. Levin, *Phil. Trans. R. Soc. Lond. B* **343**, 329 (1994).
7. J.B. Shurin, P. Amarasekare, J.M. Chase, R.D. Holt, M.F. Hoopes, M.A. Leibold, *J. Theor. Biol.* **227**, 359 (2004).
8. P. Amarasekare, *Ecol. Lett.* **6**, 1109 (2003).
9. D.W. Yu, H.B. Wilson, *Am. Nat.* **158**, 49 (2001).
10. D.E. Taneyhill, *Ecol. Monogr.* **70**, 495 (2000).
11. A.N. Kolmogorov, *Bull. Acad. Sci. USSR, Phys. Ser.* **1**, 355 (1937).
12. W. A. Johnson and R. F. Mehl, *Trans. Am. Inst. Mining and Metallurgical Engineers* **135**, 416 (1939).
13. M. Avrami, *J. Chem. Phys.* **7**, 1103 (1939); **8**, 212 (1940); **9**, 177 (1941).
14. J.D. Gunton and M. Droz, *Introduction to the Theory of Metastable and Unstable States* (Springer, Berlin, 1983),
15. G.A. Yarranton, R.G. Morrison, *J. Ecol.* **62**, 417 (1974).
16. G. Korniss, T. Caraco, *J. Theor. Biol.* **233**, 137 (2005).
17. P.A. Rikvold, H. Tomita, S. Miyashita, S.W. Sides, *Phys. Rev. E* **49**, 5080 (1994).
18. H.L. Richards, S.W. Sides, M.A. Novotny, P.A. Rikvold, *J. Magnet. Mater.* **150**, 37 (1995).
19. R.A. Ramos, P.A. Rikvold, M.A. Novotny, *Phys. Rev. B* **59**, 9053 (1999).
20. G. Korniss, M.A. Novotny, P.A. Rikvold, *J. Comput. Phys.* **153**, 488 (1999).
21. Y. Ishibashi, Y. Takagi, *J. Phys. Soc. Jpn.* **31**, 506 (1971).
22. H.M. Duiker, P.D. Beale, *Phys. Rev. B* **41**, 490 (1990).
23. E. Machado, G. M. Buendia, P. A. Rikvold, *Phys. Rev. E* (in press, 2005); arXiv: cond-mat/0411335.
24. J. Herrick, S. Sun, J. Bechhoefer, A. Bensimon, *J. Mol. Biol.* **320** 741 (2002).
25. A. Gandhi, S. Levin, S. Orszag, *J. Theor. Biol.* **200**, 121 (1999).